21

Adaptive Signal Selection Control Based on Adaptive FF Control Scheme and Its Applications to Sound Selection Systems

Hiroshi Okumura[1] and Akira Sano[2]
[1]*Research & Development Department, Medical System Division, Shimadzu Corporation*
[2]*Faculty of System Design Engineering, Keio University*
Japan

1. Introduction

Noise pollution is one of the social problems, and many researches on active noise control (ANC) or active vibration control (AVC) have been done (Tokhi & Veres, 2002). Almost all previous studies were interested in suppression of unwanted noise signals. However, actually some necessary signals should not be suppressed but transmitted and only unnecessary noise should be blocked. Therefore, a control method which can selectively attenuate only unnecessary signals is needed.

In this chapter, we will propose a novel control scheme which can transmit necessary signals (Necs) and attenuate only unnecessary signals (Unecs) selectively. The control scheme is named as Signal Selection Control (SSC) scheme.

The purpose of this chapter is to develop two types of the SSC; one is Necs-Extraction Controller which transmits only signals set as Necs, and the other is Unecs-Canceling Controller which attenuates only signals set as Unecs. The Necs-Extraction Controller was proposed by us before (Okumura & Sano, 2009), and the Unecs-Canceling Controller is newly proposed in this chapter. Results of both controllers are the same; both controllers transmit Necs and attenuate Unecs selectively, however, the design concept of each controller is different. When some Necs are known, the Necs-Extraction Controller is suitable and the Necs is set to be transmitted. On the other hand, when some Unecs are known, the Unecs-Canceling Controller is suitable and the Unecs is set to be attenuated. We can choose these two controllers according to the application systems.

The SSC is based on adaptive feedforward (FF) control schemes which were adopted in the fields of ANC and AVC due to its excellent performance of noise attenuation. In this chapter, four adaptive controllers will be introduced and characterized; (i) the filtered-X LMS controller which is a conventional approach in the adaptive FF control field (Burgess, 1981; Widrow et al, 1982), (ii) the 2-degree-of-freedom filtered-X LMS controller (Kuo, 1996, 1999), (iii) the Virtual Error controller which is proposed by one of the authors before (Kohno & Sano, 2005; Ohta & Sano, 2004), and (iv) the 2-degree-of-freedom Virtual Error controller which is also proposed by us before(Okumura & Sano, 2009).

To validate effectiveness of the proposed SSC, two applications to Sound Selection Systems (SSS) are considered as numerical simulations.

(i) First example is an application of the Necs-Extraction Controller to a smart window system of a car, which can transmit only electronic siren sound of ambulance as Necs, but block any other noises such as road noise and engine noise. Purpose of this application is to keep car room silent and safety against car accidents at the same time.
(ii) Second example is another application of the Unecs-Canceling Controller to rotating machinery such as a compressor, which can attenuate only sound of rotating motor as Unecs even when rotating speed is changing, but transmit some abnormal sound of the machinery. Purpose of this application is to keep machinery silence and detectability of machine abnormality at the same time.
Through above two numerical simulations, effectiveness of the proposed Signal Selection Control (SSC) scheme is validated.

2. Sound Selection System

In those two numerical simulations, we consider a double glazed plate system as a Sound Selection System (SSS), and develop its mathematical models.
The structure of a double glazed plate was often employed in ANC field. Two type of approaches were taken; one is 'cavity control' applying acoustic control sources in the air gap between the two plates (Sas et al, 1995; Jakob & Möser, 2003a, 2003b; Kaiser et al, 2003), and the other is 'panel control' applying vibration control sources on the radiating plate (Bao & Pan, 1997, 1998). In the cavity control approaches in which microphones and loudspeakers are usually used to sense and actuate sounds, there must be some large space to place them. Therefore, we will employ the panel control approach to realize the SSS.
For the purpose, we use piezoelectric ceramics to sense and control the vibration of plates by making use of the advantage that piezoelectric ceramics can be used as both actuator and sensor. Besides, due to its simplicity, small size, broad bandwidth, easy implementation, and efficient conversion between electrical and mechanical energy, recently, smart structures with piezoelectric actuator and sensor pairs have collected much attention (Moheimani, 2003).

2.1 Description of the SSS considered in this chapter

Fig. 1 shows the structure of the considered Sound Selection System (SSS). As shown in Fig. 1(a) and Fig. 2, the SSS is a double glazed plate whose distance between two plates is 34mm, and a piezoelectric reference sensor and error sensor are attached on the 1st and 2nd plates to sense each plate's vibration respectively. A piezoelectric actuator is also attached on the 2nd plate to control the 2nd plate's vibration.
Fig. 1(b) describes the position of piezoelectric actuators or sensors on each plate, and the reference sensors, error sensors and control actuators are patched on the same position of each plate's surface (this positioning is so called 'collocation'). There are two patches; one is for actuation or sensing of vibration along one axis, the other is for along the other axis.

2.2 Control scheme of the SSS

Fig. 2 and Fig. 3 show a schematic diagram for adaptive control of the SSS.
As shown in the Fig. 2 and Fig. 3, SSS is a double glazed plate system, and in the SSS, the adaptive SSC operates to control transmitting sound through the double glazed plate by controlling the 2nd plate’s vibration using piezoelectric actuator on it, according to information of 1st plate’s vibration sensed by piezoelectric sensor on it.

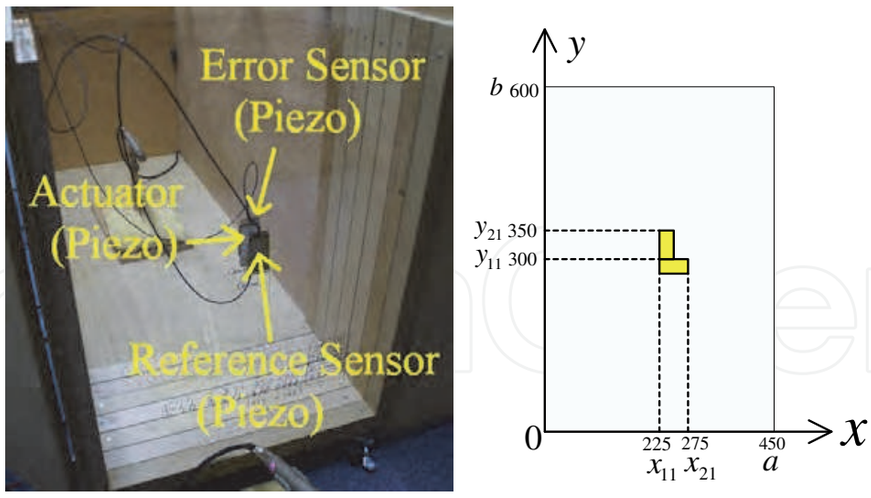

(a) Setup of the SSS (b) Position of actuator and sensor

Fig. 1. Structure of the considered Sound Selection System

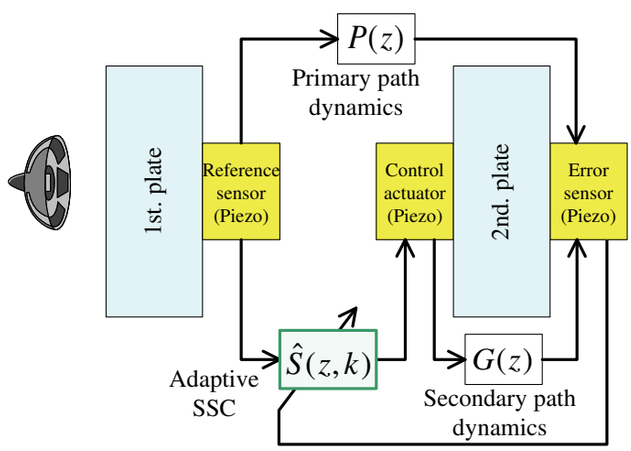

Fig. 2. Schematic diagram of the considered SSS

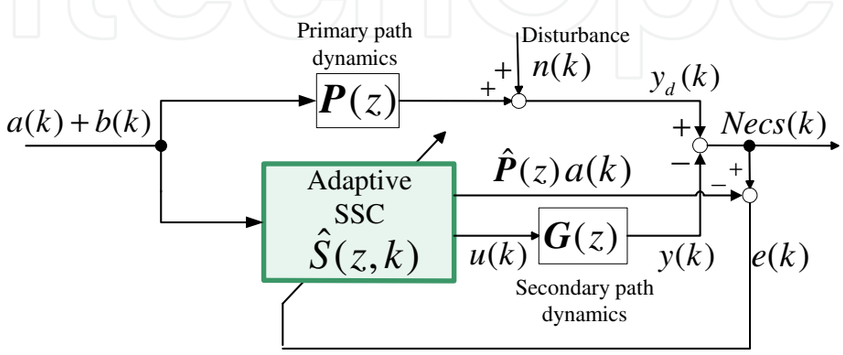

Fig. 3. Block diagram for the proposed Signal Selection Control scheme

A path from the reference sensor to error sensor is referred to as the primary path dynamics $P(z)$, and a path from the control actuator to error sensor as the secondary path dynamics $G(z)$. Let $a(k)$ be necessary signals to be transmitted, $b(k)$ be other unnecessary noise to be suppressed, $n(k)$ the disturbance in the primary path which cannot be sensed by the reference sensor, $u(k)$ the control voltage input to the piezo actuator, $Necs(k)$ the transmitted vibration signal sensed by the error sensor on the 2nd plate, and $e(k)$ the error signal used to adjust the adaptive controller $\hat{S}(z,k)$. $y_d(k)$ and $y(k)$ denote the vibration signal excited in the primary and secondary path dynamics respectively, which are not available separately.

The purpose of the adaptive controller $\hat{S}(z,k)$ is to transmit only necessary sound $a(k)$, but blocks any other unnecessary noises $b(k)$ and disturbances $n(k)$ in the primary path. As mentioned later, $\hat{S}(z,k)$ is referred to as the Signal Selection Controller, and it is composed of an extractor which can extract only desired signals, and of an adaptive controller which can force the error $e(k)$ to zero even when the primary and secondary path dynamics are both unknown and the unknown disturbance $n(k)$ is added to the primary path.

In the section 3, modelling of the primary and secondary path dynamics is described, and in the section 4, design of the adaptive SSC is explained.

3. System modelling for numerical simulations

This section gives the model description for the primary path dynamics $P(z)$ and the secondary path dynamics $G(z)$ in Fig. 2 and Fig. 3.

At first, necessary physical parameters for the plates and piezoelectric ceramics are listed in Table 1 and Table 2, and the notations are used in modeling of the path dynamics. In the Table 2, the conversion factor κ is described as follows (Moheimani & Fleming, 2005).

$$\kappa = \frac{3d_{31}IE_bE_p\left\{\left(\frac{h}{2}+h_p\right)^2-\left(\frac{h}{2}\right)^2\right\}}{2h_p\left[E_p\left\{\left(\frac{h}{2}+h_p\right)^3-\left(\frac{h}{2}\right)^3\right\}+E_b\left(\frac{h}{2}\right)^3\right]} \tag{1}$$

Parameters	Characters	Values	Units
Width	a	0.450	[m]
Height	b	0.600	[m]
Thichness	h	$0.5\text{x}10^{-3}$	[m]
Density	ρ	$1.18\text{x}10^{3}$	[kg/m^3]
Young's modulus	E	$0.21\text{x}10^{10}$	[N/m^2]
Poisson's ratio	υ	0.16	-
Moment of inertia of area	I	$4.7\text{x}10^{-12}$	[m^4]

Table 1. Parameters of the plates (Polycarbonate)

Parameters	Characters	Values	Units
Length	L_p	49.999x10^{-3}	[m]
Width	W_p	24.993x10^{-3}	[m]
Thichness	h_p	0.4549x10^{-3}	[m]
Capacitance	C_p	298.200x10^{3}	[F]
Young's modulus	E_p	6.2x10^{10}	[N/m^2]
Strain coefficent	d_{31}	-266x10^{-12}	[m/V]
Conversion factor	κ	-9.655x10^{-6}	$[(N \cdot m)/V]$

Table 2. Parameters of the piezoelectric ceramics (PZT)

3.1 Modelling of the primary path dynamics P(z)

The primary path dynamics $P(z)$ is a path from the reference sensor to the error sensor, as shown in Fig. 2. As mentioned above, if the distance between two plates is set to 34mm and the sampling frequency is chosen as 50kHz (0.02ms), then it takes 5 sampling instants for the primary sound to propagate the gap distance. In the case, the primary path dynamics can be expressed as a simple delay and constant multiplication, described as follows.

$$P(z) = p_1 z^{-5}, \ (0 < p_1 \le 1) \tag{2}$$

Where z^{-1} means the time delay operator.

3.2 Modelling of the secondary path dynamics G(z)

The secondary path dynamics $G(z)$ is a path from the control actuator to the error sensor, as shown in Fig. 2. A dynamic model of $G(z)$ is described as a transfer function from the control voltage input for the actuator to the error sensor voltage sensing the vibration of the 2nd plate. So, the modeling of $G(z)$ needs analysis how the piezoelectric actuator excites vibration onto the plate by the input voltage and how the piezoelectric sensor detects the vibration.

The plate's equation of motion is described by a distributed parameter system expressed as

$$\rho h \frac{\partial^2 w(x,y,t)}{\partial t^2} + D\left(\frac{\partial^4 w(x,y,t)}{\partial x^4} + \frac{\partial^4 w(x,y,t)}{\partial x^2 \partial y^2} + \frac{\partial^4 w(x,y,t)}{\partial y^4}\right) = F(x,y,t), \tag{3}$$

where $w(x,y,t)$ is the displacement of the plate along z-axis and $F(x,y,t)$ is the external force at the position (x,y) and time t, and D is the bending rigidity. The external force $F(x,y,t)$ by the piezoelectric actuator as the moment is expressed as

$$F(x,y,t) = \frac{\partial^2 M(x,y,t)}{\partial x^2} + \frac{\partial^2 M(x,y,t)}{\partial y^2}, \tag{4}$$

where $M(x,y,t)$ is the moment at the position (x,y) and time t. Thus, the equation of motion is rewritten as

$$\rho h \frac{\partial^2 w(x,y,t)}{\partial t^2} + D\left(\frac{\partial^4 w(x,y,t)}{\partial x^4} + \frac{\partial^4 w(x,y,t)}{\partial x^2 \partial y^2} + \frac{\partial^4 w(x,y,t)}{\partial y^4} \right) = \frac{\partial^2 M(x,y,t)}{\partial x^2} + \frac{\partial^2 M(x,y,t)}{\partial y^2}. \tag{5}$$

Besides, the moment can be expressed by using the actuator voltage input $v_a(t)$ as

$$M(x,y,t) = \kappa v_{ai}(t), \tag{6}$$

where κ is defined by (1), and the subscript i denotes the actuator number in a multi-channel case using multiple actuators.

On the other hand, the piezoelectric sensor generates voltage by its bending deformation, described as

$$v_{sj}(t) = \frac{d_{31} E_p W_p}{C_p} \int_0^b \int_0^a \left(\varepsilon_x + \varepsilon_y \right) dxdy, \tag{7}$$

where $v_{sj}(t)$ is the sensor voltage and subscript j means the sensor number in a multi-channel case using multiple sensors, and ε is the strain of the piezoelectric sensor generated by bending of the plate (Moheimani & Fleming, 2005).

As a result, from (5), (6) and (7), it follows that the transfer function $G(s)$ from the i-th actuator voltage $v_{ai}(t)$ to the j-th sensor voltage $v_{sj}(t)$ is given by

$$G(s) = \frac{V_{sj}(s)}{V_{ai}(s)} = -\frac{\kappa d_{31} E_p W_p \left(\frac{h}{2} + h_p \right)}{C_p \rho h} \cdot \sum_{k=1}^{\infty} \frac{\left(\Psi_{kj} + \Phi_{kj} \right)\left(\Psi_{ki} + \Phi_{ki} \right)}{\left(\int_0^b \int_0^a W_k^2(x,y) dxdy \right)\left(s^2 + 2\varsigma_k \omega_k s + \omega_k^2 \right)}, \tag{8}$$

where $V_{ai}(s)$, $V_{sj}(s)$ are the Laplace transform of $v_{ai}(t)$, $v_{sj}(t)$ respectively, $W_k(x,y)$ is the eigen modal function of the plate, and the subscript k denotes the modal number, ς_k, ω_k are the damping ratio and eigen frequency of k-th mode respectively, and Ψ, Φ are calculated from the modal function at the location of the piezoelectric patches along x-axis and y-axis respectively. In adaptive controller design in numerical simulation, we use a truncated model within 30th modes.

Finally, we obtain a discrete-time FIR model $G(z)$ by the impulse invariance method, that is, by sampling the impulse response of the continuous-time model $G(s)$. As a result, $G(z)$ is given as an FIR model expression as

$$G(z) = \sum_{n=0}^{L_g} g_n z^{-n}, \tag{9}$$

where g_n is the impulse response coefficient at n-th sample, and L_g is the filter length of FIR model $G(z)$. g_0 becomes 0 because the transfer function is strictly proper.

It should be noticed that the secondary path dynamics (8) involves parameter uncertainties in its mathematical model, and that is a reason why the adaptive control approach is useful.

4. Design of adaptive Signal Selection Controller

The purpose of the adaptive Signal Selection Controller (SSC) $\hat{S}(z,k)$ for the SSS in Fig. 2 and Fig. 3 is to transmit only the necessary signals (Necs) and cancel any other unnecessary noise (Unecs) and the disturbance. In this section, it will be described how to realize the adaptive SSC $\hat{S}(z,k)$ which is composed of an extractor and an adaptive controller.
In the section 4.1, at first, principle of the adaptive SSC is explained.
And in the section 4.2, design of the extractor which is a component of the SSC is shown.
Next, in the section 4.3, design of the adaptive controller which is another component of the SSC is summarized.
Finally, in the section 4.4, overall structure of the SSC is described.

4.1 Principle of the adaptive Signal Selection Control scheme

Two types of the SSC is introduced; one is Necs-Extraction Controller which transmit only signals set as Necs as shown in Fig. 4, and the other is Unecs-Canceling Controller which attenuate only signals set as Unecs as shown in Fig. 5. Results of both controllers are the same; both controllers transmit Necs and attenuate Unecs selectively, however, the design concept of each controller is different. When some Necs are known, we choose the Necs-Extraction Controller and set the Necs to be transmitted. On the other hand, when some Unecs are known, we choose the Unecs-Canceling Controller and set the Unecs to be attenuated.

4.1.1 Principle of Necs-Extraction Controller

Fig. 4 shows the schematic diagram of the Necs-Extraction Controller.

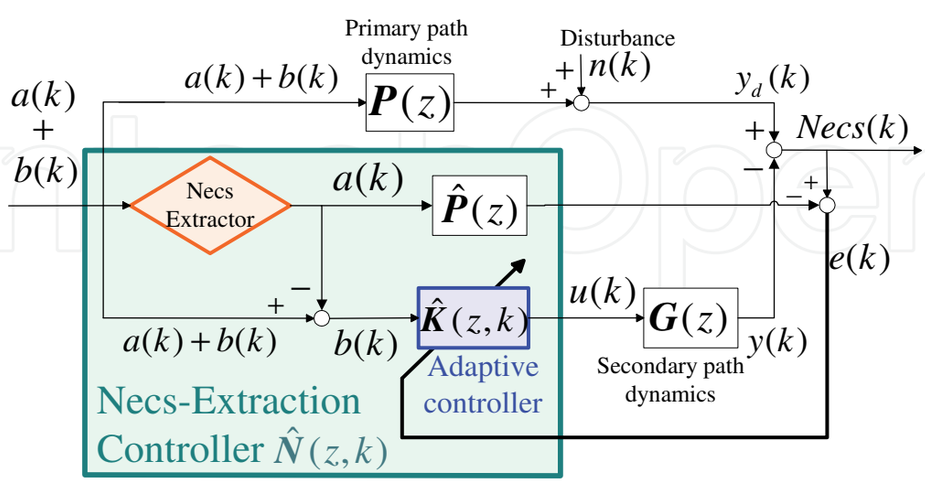

Fig. 4. Schematic diagram of the Necs-Extraction Controller (One of the SSC)

As mentioned, the SSC is composed of an extractor and an adaptive controller. In Fig. 4, $a(k)$ is a necessary signal (Necs), and $b(k)$ is an unnecessary noise (Unecs). $Necs(k)$ is the

transmitted vibration signal sensed by the error sensor on the 2nd plate, $e(k)$ is the error signal used to adjust the adaptive controller $\hat{K}(z,k)$, and $\hat{P}(z)$ is an identified model of the primary path dynamics $P(z)$.

The main operations of the Necs-Extraction Controller $\hat{N}(z,k)$ are summarized as follows;

1. The extractor extracts only the necessary signal $a(k)$.
2. Next, $a(k)$ is subtracted from the input signal to the adaptive controller $\hat{K}(z,k)$.
3. Then, $\hat{K}(z,k)$ works to attenuate only the unnecessary signal $b(k)$.
4. Then, $\hat{K}(z,k)$ is adjusted to force $e(k)$ into zero.

The above procedure is executed simultaneously in on-line manner.

The canceling error $e(k)$ is expressed as

$$e(k) = Necs(k) - \hat{P}(z)a(k), \tag{10}$$

therefore, if $e(k) \to 0$ then $Necs(k) \to \hat{P}(z)a(k)$. Thus, if $a(k) \to 0$ then $Necs(k) \to 0$, and if $a(k)$ is the necessary signal then $Necs(k)$ converges to the necessary signal through the primary path dynamics. That is the principle of the proposed Necs-Extraction Controller $\hat{N}(z,k)$.

4.1.2 Principle of Unecs-Canceling Controller

Fig. 5 shows the schematic diagram of the Unecs-Canceling Controller.

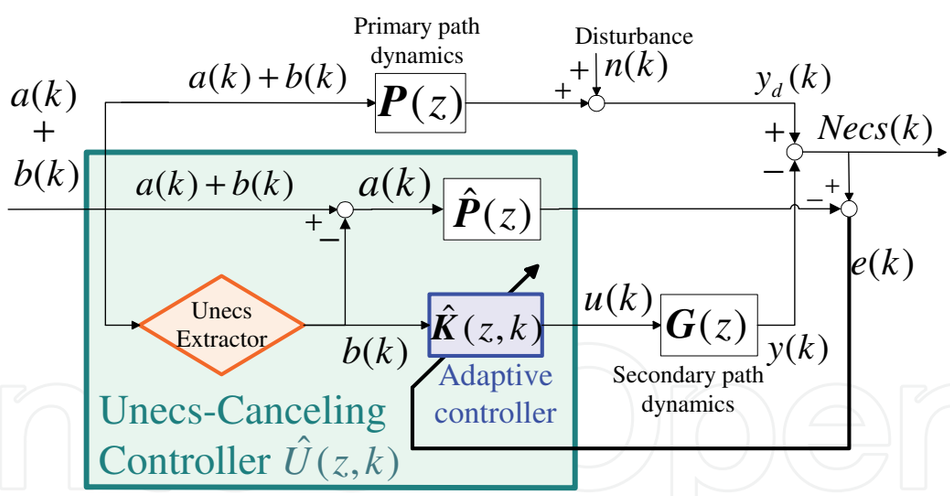

Fig. 5. Schematic diagram of the Unecs-Canceling Controller (One of the SSC)

The principle of the Unecs-Canceling Controller is almost the same as the Necs-Extraction Controller. Difference between two controllers is how to make input signal to the adaptive controller $\hat{K}(z,k)$. In the Necs-Extraction Controller, the input signal $b(k)$ is made by subtraction of $a(k)$ (which is extracted by the Necs Extractor) from $a(k)+b(k)$, however, in the Unecs-Canceling Controller, $b(k)$ is directly made by the Unecs Extractor.

The main operations of the Unecs-Canceling Controller $\hat{U}(z,k)$ are summarized as follows;

1. The extractor extracts only the unnecessary signal $b(k)$.
2. Next, $\hat{K}(z,k)$ works to attenuate only the unnecessary signal $b(k)$.

3. Then, $\hat{K}(z,k)$ is adjusted to force $e(k)$ into zero.

The above procedure is executed simultaneously in on-line manner.

The canceling error $e(k)$ is expressed as same as (10), therefore, if $e(k) \to 0$ then $Necs(k) \to \hat{P}(z)a(k)$. Thus, whether $b(k)$ is exist or not, $b(k)$ is not transmitted and $Necs(k)$ converges to the necessary signal through the primary path dynamics. That is the principle of the proposed Unecs-Canceling Controller $\hat{U}(z,k)$.

In the following sections, we show how to design the extractor extracting only desired signal with varying frequencies, and how to update the adaptive controller $\hat{K}(z,k)$ so that the canceling error can be forced into zero.

4.2 Design of the extractor

The purpose of the extractor is to extract the desired signal by tracking only frequencies of desired signals even in the presence of frequency variations. It should be noticed that Necs Extractor and Unecs Extractor is the same; when the desired signal is Necs $a(k)$, the extractor is named as Necs Extractor, and when the desired signal is Unecs $b(k)$, the extractor is named as Unecs Extractor.

The extractor is a new adaptive filter with tacking ability to selected frequencies, which is composed of a harmonics synthesizer and a judging synthesizer as shown in Fig. 6. The harmonics synthesizer estimates frequency and amplitude of all sinusoidal signals in the input signals. And then, the judging synthesizer judges whether each sinusoidal signal is necessary or not. Depend on the purpose of the extractor, the judging synthesizer should be modified.

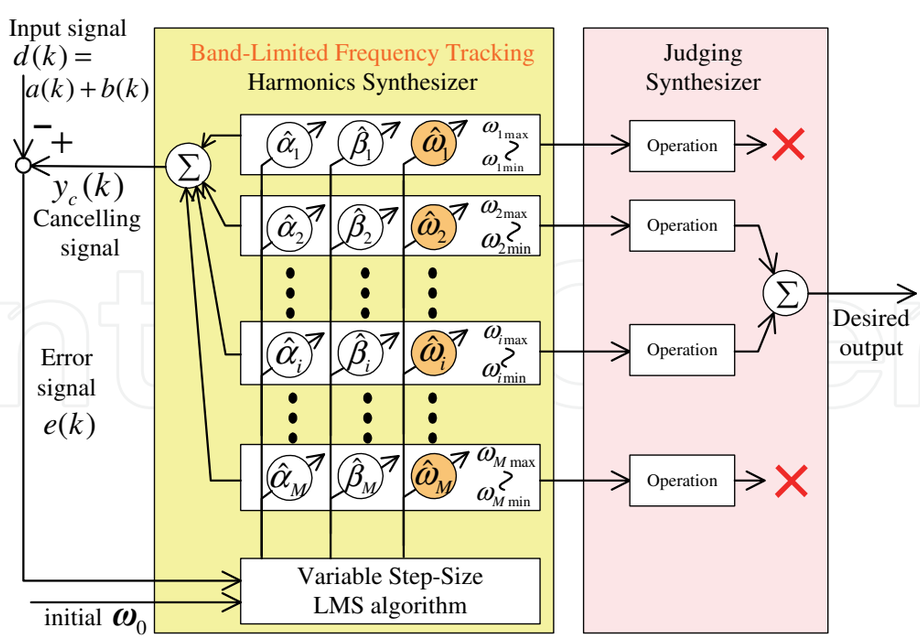

Fig. 6. Schematic diagram of the extractor

The algorithm for the extractor is based on the DXHS algorithm (Shimada et al, 1999), but we improve the operation performance by adding new abilities and functions; (i)

improvement of readiness for frequency estimation by introduction of a variable step-size algorithm, (ii) limitation of frequency-estimation bandwidth, and (iii) judging system whether one signal is necessary or not.

The main procedure of the extractor is summarized as follows;

1. Estimation of the amplitudes α, β and frequency ω of each sinusoidal signal composing the input signal $d(k)$ adaptively by using the error signal $e(k) = y_c(k) - d(k)$, where $y_c(k)$ is the canceling signal for $d(k)$ which is the sum of all estimated sinusoidal signal.
2. Judging whether each estimated sinusoidal signal is necessary or not.
3. Synthesizing only necessary signals to be a desired output.

In the Fig. 6, the Extractor estimates M sinusoidal signals, and each estimation bandwidth is limited from $\omega_{\min}$ to $\omega_{\max}$. Then, 2nd and i th signal are judged to be necessary.

The canceling signal $y_c(k)$ is synthesized as

$$y_c(k) = \sum_{i=1}^{M} \left(\hat{\alpha}_i(k) \cos(\hat{\Omega}_i(k)) + \hat{\beta}_i(k) \sin(\hat{\Omega}_i(k)) \right) \tag{11}$$

$$\hat{\omega}_i(k)kT \equiv \hat{\Omega}_i(k) = \hat{\Omega}_i(k-1) + \hat{\omega}_i(k)T, \ (-\pi \le \hat{\Omega}_i(k) < \pi), \tag{12}$$

and the amplitudes and frequencies are estimated adaptively by the adaptation laws as;

$$\hat{\alpha}_i(k+1) = \hat{\alpha}_i(k) - 2\mu e(k) \cos(\hat{\Omega}_i(k)) \tag{13}$$

$$\hat{\beta}_i(k+1) = \hat{\beta}_i(k) - 2\mu e(k) \sin(\hat{\Omega}_i(k)) \tag{14}$$

$$\hat{\omega}_i(k+1) = \tilde{\omega}_i(k) - 2\mu_\omega(k) T e(k) \cdot \left[-\hat{\alpha}_i(k) \sin(\hat{\Omega}_i(k)) + \hat{\beta}_i(k) \cos(\hat{\Omega}_i(k)) \right] \tag{15}$$

$$\tilde{\omega}_i(k) = \begin{cases} \omega_{i\max} & (\omega_{i\max} \le \omega_i(k)) \\ \omega_i(k) & (\omega_{i\min} < \omega_i(k) < \omega_{i\max}) \\ \omega_{i\min} & (\omega_i(k) \le \omega_{i\min}) \end{cases} \tag{16}$$

$$\mu_\omega(k) = (\mu_{\max} - \mu_{\min}) \frac{\left(\sum_{n=k-N}^{k} |e(n)| \right) / N}{\rho + \left(\sum_{n=k-N}^{k} |d(n)| \right) / N} + \mu_{\min}, \tag{17}$$

where μ is a constant step size in the adaptation of amplitudes and $\mu_\omega(k)$ is a variable step size in the adaptation of frequencies given in (17) where $\mu_{\max}$ and $\mu_{\min}$ are maximum and minimum value of step size which are design parameters, ρ is a small positive constant employed to avoid division by zero, and N is the sample number to be used for moving average.

4.2.1 Necs Extractor for ambulance's siren sound

In this chapter, we consider the Necs-Extraction Controller which extracts the siren sound of ambulance. So in this section, design of the judging synthesizer for siren sound is described.

In Japan the siren signal of an ambulance consists of 960Hz sound (pi) and 770Hz sound (po), and the two sounds repeat one after the other at 0.65s cycle. The two frequencies change by the Doppler effect from 900Hz to 1060Hz for pi and from 700Hz to 850Hz for po respectively, when the maximum relative speed against an ambulance is 120km/h. We also consider a situation when another unnecessary noise exists in a band of the varying siren frequencies, for instance, unnecessary sinusoidal noise with 900Hz.

To judge the siren signal, we use the frequency information mainly and amplitude information supplementarily. To be more specific, the frequency information used for siren judgement is as follows;

1. 'pi' is 960Hz sound and 'po' is 770Hz sound.
2. The two sounds vary in the same ratio by the Doppler effect.
3. The two sounds alternate in 0.65s cycle.

The judgement flow is given as follows;

1. Estimate the frequency of likely 'pi' (or 'po').
2. Calculate the frequency of the alternative, that is, 'po' (or 'pi') by using the Doppler effect.
3. If there is a sound 0.65s before whose frequency is a similar one calculated in step 2, it must be the siren signal.
4. Output the signals judged as the siren.

By above four steps, the judging synthesizer judges the siren signals.

4.2.2 Unecs extractor for compressor's motor sound

In this chapter, we consider the Unecs-Canceling Controller which attenuates the rotating motor's sound of a compressor. So in this section, design of the judging synthesizer for compressor's motor sound is described.

In this case, information of rotation order signal can be used. In the case of using AC servo motor, rotation orders like target frequency is sent to the motor. Using this target frequency information, the judging synthesizer can extract only rotating motor sound with tracking to the rotating frequency variation.

4.3 Design of the adaptive controllers

In the Fig. 4 and Fig. 5, the adaptive controller $\hat{K}(z,k)$ needs to update the parameter of the controller itself so that the canceling error $e(k)$ can be forced into zero.

In this section, four adaptive controllers are introduced and characterized; (i) the filtered-X LMS controller which is a conventional approach in the adaptive FF control field (Burgess, 1981; Widrow et al, 1982), (ii) the 2-degree-of-freedom filtered-X LMS controller (Kuo, 1996, 1999), (iii) the Virtual Error controller which is proposed by one of the authors before (Kohno & Sano, 2005; Ohta & Sano, 2004), and (iv) the 2-degree-of-freedom Virtual Error controller which is also proposed by us before (Okumura & Sano, 2009). The following section gives summary for these controllers, brief description about controller (i), (ii) and (iii), and detail information about controller (iv).

4.3.1 Summary for four adaptive controllers

In the fields of ANC and AVC, adaptive feedforward control schemes were adopted due to excellent performance of noise attenuation. Almost previous works employed various type of filtered-x (FX) algorithms (Burgess, 1981; Widrow et al, 1982), but they are not stability-assured

since the canceling error is directly used in adaptive algorithms for updating controller parameters. One of the authors proposed the Virtual Error (VE) approach which does not use the canceling error directly but a virtual error in the adaptation, and is locally stability-assured (Kohno & Sano, 2005; Ohta & Sano, 2004). However, since both FX and VE approaches are used in the feedforward (FF) control, they cannot attenuate the effects of unknown disturbances to the primary path dynamics, which cannot be sensed by a reference sensor.
To attenuate the disturbance noise in the primary path, feedback (FB) control should be additionally employed. Previously we proposed a two degree-of-freedom (2DF) control scheme consisting of an adaptive FF controller and a fixed but robust FB controller (Okumura et al, 2008), but the approach needs nominal information on the secondary path dynamics and the performance sometime becomes degraded due to its model uncertainty. A 2DF control scheme consisting of adaptive FF and FB controllers based on 2DF filtered-X algorithm has also been studied (Kuo, 1996, 1999), but can hardly adjust the two adaptive controllers simultaneously. So, we proposed a novel VE approach for updating all the parameters of the both adaptive FF and FB controllers simultaneously in on-line manner, which is the 2DF Virtual Error controller (Okumura & Sano, 2009).

4.3.2 Filterd-X LMS (FX) controller

Fig. 7 shows block diagram of the filtered-X LMS (FX) controller. And the adaptation law for the controller parameters is as follows (Burgess, 1981; Widrow et al, 1982). (Meanings of characters are described in section 4.3.5, so see detail in the section 4.3.5.)

$$\hat{\boldsymbol{\theta}}_C(k+1) = \hat{\boldsymbol{\theta}}_C(k) + \mu_C e(k) G(z) \boldsymbol{\xi}(k) \tag{18}$$

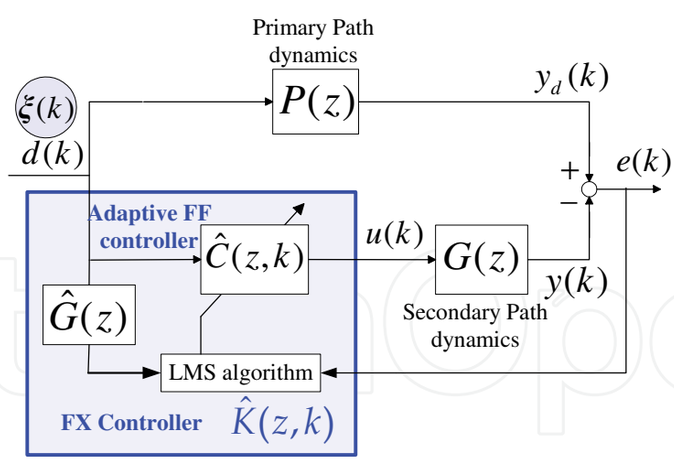

Fig. 7. Block diagram of the filtered-X LMS controller

4.3.3 2-degree-of-freedom filtered-X LMS (2DF-FX) controller

Fig. 8 shows block diagram of the 2-degree-of-freedom filtered-X LMS (2DF-FX) controller. And the adaptation laws for the controller parameters are as follows (Kuo, 1996, 1999). (Meanings of characters are described in section 4.3.5, so see detail in the section 4.3.5.)

$$\hat{\boldsymbol{\theta}}_C(k+1) = \hat{\boldsymbol{\theta}}_C(k) + \mu_C e(k) G(z) \boldsymbol{\xi}(k) \tag{19}$$

$$\hat{\boldsymbol{\theta}}_B(k+1) = \hat{\boldsymbol{\theta}}_B(k) + \mu_B e(k) G(z) \boldsymbol{\eta}(k) \tag{20}$$

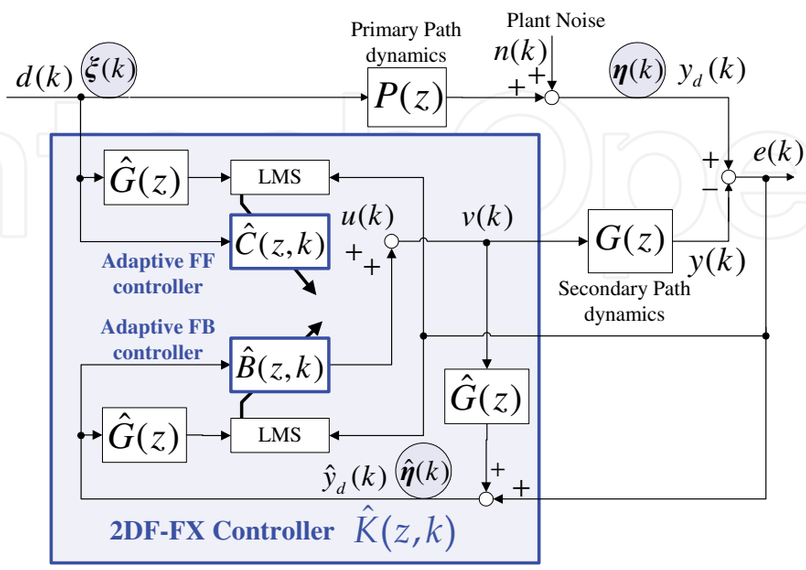

Fig. 8. Block diagram of the 2-degree-of-freedom filtered-X LMS controller

4.3.4 Virtual Error (VE) controller

Fig. 9 shows block diagram of the Virtual Error (VE) controller. And the adaptation laws for the controller parameters are as follows (Kohno & Sano, 2005; Ohta & Sano, 2004). (Meanings of characters are described in section 4.3.5, so see detail in the section 4.3.5.)

$$\hat{\boldsymbol{\theta}}_D(k+1) = \hat{\boldsymbol{\theta}}_D(k) + \mu_D e_A(k) \boldsymbol{\xi}(k) \tag{21}$$

$$\hat{\boldsymbol{\theta}}_H(k+1) = \hat{\boldsymbol{\theta}}_H(k) + \mu_H e_A(k) \boldsymbol{\varsigma}(k) \tag{22}$$

$$\hat{\boldsymbol{\theta}}_C(k+1) = \hat{\boldsymbol{\theta}}_C(k) + \mu_C e_B(k) \boldsymbol{\varphi}(k) \tag{23}$$

4.3.5 2-degree-of-freedom Virtual Error (2DF-VE) controller

The main purpose of the adaptive controller block $\hat{K}(z,k)$ is to force the error signal $e(k)$ into zero even in the presence of uncertainties in the path dynamics and disturbance. In this section, we propose a 2-degree-of-freedom virtual error (2DF-VE) approach to update the parameters of four adaptive filters shown in Fig. 10.

The original version of the virtual error (VE) approach was proposed by one of the authors (Kohno & Sano, 2005; Ohta & Sano, 2004), but it could not treat with the unknown disturbance $n(k)$. In the new VE approach, by introducing the adaptive feedback (FB) controller $\hat{B}(z,k)$, we can also suppress the disturbance effects by $n(k)$. Hence this scheme is referred to as the 2DF-VE algorithm, since it consists of the adaptive feedforward (FF) controller $\hat{C}(z,k)$ and the adaptive feedback (FB) controller $\hat{B}(z,k)$.

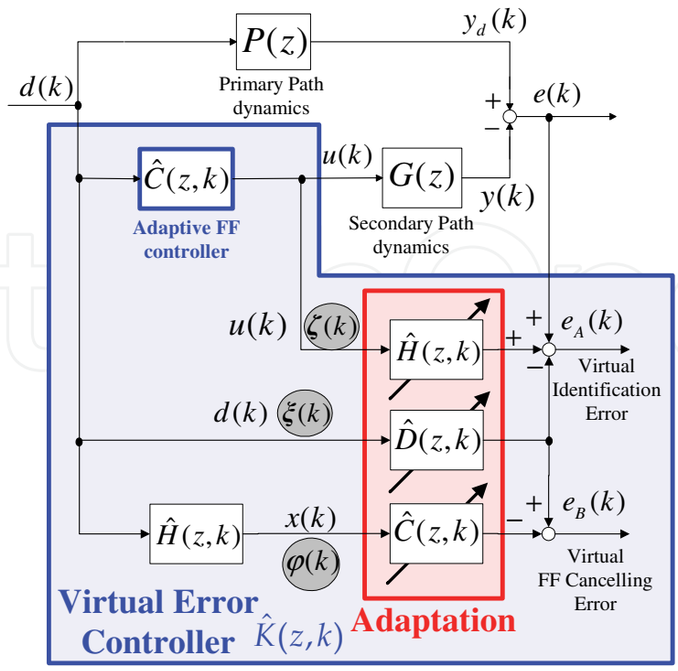

Fig. 9. Block diagram of the Virtual Error controller

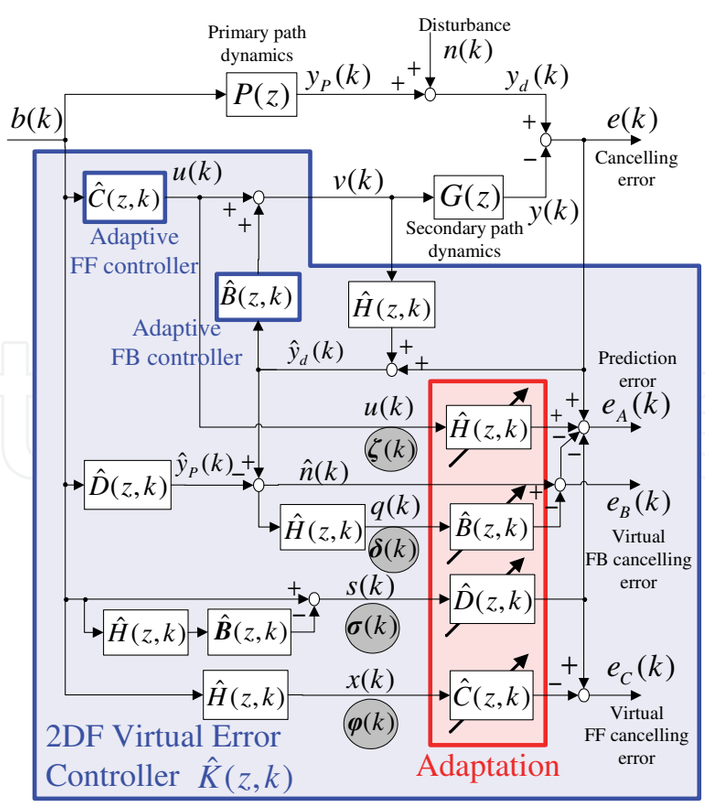

Fig. 10. Block diagram of the 2-degree-of-freedom Virtual Error controller

As shown in Fig. 10, we introduce the virtual FB canceling error $e_B(k)$ and the virtual FF canceling error $e_C(k)$ as well as the prediction error $e_A(k)$ to update the parameters of the four FIR adaptive filters $\hat{B}(z,k)$, $\hat{C}(z,k)$, $\hat{H}(z,k)$ and $\hat{D}(z,k)$, which are given as

$$\hat{D}(z,k) = \hat{d}_1(k)z^{-1} + \hat{d}_2(k)z^{-2} + \cdots + \hat{d}_{L_d}(k)z^{-L_d} \tag{24}$$

$$\hat{H}(z,k) = \hat{h}_1(k)z^{-1} + \hat{h}_2(k)z^{-2} + \cdots + \hat{h}_{L_h}(k)z^{-L_h} \tag{25}$$

$$\hat{B}(z,k) = \hat{b}_1(k)z^{-1} + \hat{b}_2(k)z^{-2} + \cdots + \hat{b}_{L_b}(k)z^{-L_b} \tag{26}$$

$$\hat{C}(z,k) = \hat{c}_1(k)z^{-1} + \hat{c}_2(k)z^{-2} + \cdots + \hat{c}_{L_c}(k)z^{-L_c}. \tag{27}$$

Let the parameter vector of each adaptive filter be defined by

$$\hat{\boldsymbol{\theta}}_D(k) = \left(\hat{d}_1(k), \hat{d}_2(k), \cdots, \hat{d}_{L_d}(k)\right)^T \tag{28}$$

$$\hat{\boldsymbol{\theta}}_H(k) = \left(\hat{h}_1(k), \hat{h}_2(k), \cdots, \hat{h}_{L_h}(k)\right)^T \tag{29}$$

$$\hat{\boldsymbol{\theta}}_B(k) = \left(\hat{b}_1(k), \hat{b}_2(k), \cdots, \hat{b}_{L_b}(k)\right)^T \tag{30}$$

$$\hat{\boldsymbol{\theta}}_C(k) = \left(\hat{c}_1(k), \hat{c}_2(k), \cdots, \hat{c}_{L_c}(k)\right)^T. \tag{31}$$

Let the corresponding regressor vector be defined as:

$$\boldsymbol{\sigma}(k) = \left(s(k-1), s(k-2), \cdots, s(k-L_d)\right)^T \tag{32}$$

$$\boldsymbol{\varsigma}(k) = \left(u(k-1), u(k-2), \cdots, u(k-L_h)\right)^T \tag{33}$$

$$\boldsymbol{\delta}(k) = \left(q(k-1), q(k-2), \cdots, q(k-L_b)\right)^T \tag{34}$$

$$\boldsymbol{\varphi}(k) = \left(x(k-1), x(k-2), \cdots, x(k-L_c)\right)^T. \tag{35}$$

The principle of the 2DF-VE controller is not to force the error $e(k)$ directly into zero, but to force it indirectly by making three virtual errors $e_A(k), e_B(k), e_C(k)$ zero. That is why we call the approach as the virtual error method.

In Fig. 10, $e_A(k)$ is a prediction error, and if the signals have the PE property then the identification of $P(z)$ and $G(z)$ can be completely done. However, the PE property is not required but we only need the convergence of $e_A(k)$ to zero. Therefore, the parameters in $\hat{D}(z,k)$ and $\hat{H}(z,k)$ are adjusted adaptively so that $e_A(k)$ becomes zero. $e_B(k)$ is a virtual FB canceling error, and the parameters of the adaptive FB controller $\hat{B}(z,k)$ are updated to

cancel the estimated plant noise $\hat{n}(k)$ so that $e_B(k)$ converges to zero. $e_C(k)$ is a virtual FF canceling error, and the parameters of the adaptive FF controller $\hat{C}(z,k)$ are also updated so that $e_C(k)$ converges to zero. These errors are related with the signals in Fig. 10 and can be expressed as follows:

$$e_A(k) = e(k) - (\hat{D} - \hat{D}\hat{B}\hat{H} - \hat{H}\hat{C})d(k) - e_B(k) \tag{36}$$

$$e_B(k) = (1 - \hat{B}\hat{H})\hat{n}(k) \tag{37}$$

$$e_C(k) = (\hat{D} - \hat{D}\hat{B}\hat{H} - \hat{C}\hat{H})d(k), \tag{38}$$

then it gives that

$$e_A(k) + e_B(k) + e_C(k) = e(k) + (\hat{H}\hat{C} - \hat{C}\hat{H})d(k). \tag{39}$$

If the parameters of $\hat{H}(z,k)$ and $\hat{C}(z,k)$ converge to constants, then it gives that

$$e_A(k) + e_B(k) + e_C(k) = e(k). \tag{40}$$

Therefore, if $e_A(k), e_B(k), e_C(k)$ are separately forced to zero, then it holds that $e(k)$ converges to zero.

To derive the adaptive algorithm which forces the errors $e_A(k), e_B(k), e_C(k)$ separately to zero, we first describe the error systems relating each error with the parameter errors as

$$\begin{aligned} e_A(k) &= (P - \hat{D})s(k) - (G - \hat{H})u(k) + \alpha(k) \\ &= \left[\boldsymbol{\theta}_{D*} - \hat{\boldsymbol{\theta}}_D(k)\right]^T \boldsymbol{\sigma}(k) - \left[\boldsymbol{\theta}_{H*} - \hat{\boldsymbol{\theta}}_H(k)\right]^T \boldsymbol{\varsigma}(k) + \alpha(k) \end{aligned} \tag{41}$$

$$e_B(k) = \left(\frac{1}{\hat{H}} - \hat{B}\right)q(k) + \beta(k) = \left[\boldsymbol{\theta}_{B*} - \hat{\boldsymbol{\theta}}_B(k)\right]^T \boldsymbol{\delta}(k) + \beta(k) \tag{42}$$

$$e_C(k) = \left(\frac{\hat{D} - \hat{D}\hat{B}\hat{H}}{\hat{H}} - \hat{C}\right)x(k) + \gamma(k) = \left[\boldsymbol{\theta}_{C*} - \hat{\boldsymbol{\theta}}_C(k)\right]^T \varphi(k) + \gamma(k) \tag{43}$$

where $\alpha(k), \beta(k), \gamma(k)$ are uncertain terms due to unmodelled dynamics, and the subscript * denotes the true value of each adaptive filter.

As a result, we can derive the robust adaptation laws by using ε_1-modification approach (Narendra & Annaswarny, 1986) as follows;

$$\hat{\boldsymbol{\theta}}_D(k+1) = \left(1 - \gamma_A \left|\frac{e_A(k)}{m_A(k)}\right|\right)\hat{\boldsymbol{\theta}}_D(k) + \frac{\mu_D e_A(k)\boldsymbol{\sigma}(k)}{m_A^2(k)} \tag{44}$$

$$\hat{\boldsymbol{\theta}}_H(k+1) = \left(1 - \gamma_A \left|\frac{e_A(k)}{m_A(k)}\right|\right)\hat{\boldsymbol{\theta}}_H(k) + \frac{\mu_H e_A(k)\boldsymbol{\varsigma}(k)}{m_A^2(k)} \tag{45}$$

$$\hat{\boldsymbol{\theta}}_B(k+1) = \left(1 - \gamma_B \left|\frac{e_B(k)}{m_B(k)}\right|\right)\hat{\boldsymbol{\theta}}_B(k) + \frac{\mu_B e_B(k)\boldsymbol{\delta}(k)}{m_B^2(k)} \tag{46}$$

$$\hat{\boldsymbol{\theta}}_C(k+1) = \left(1 - \gamma_C \left|\frac{e_C(k)}{m_C(k)}\right|\right)\hat{\boldsymbol{\theta}}_C(k) + \frac{\mu_C e_C(k)\varphi(k)}{m_C^2(k)} \tag{47}$$

$$m_A(k+1) = \mu_{mA} m_A(k) + g_A \max\left(\left\|\begin{matrix}\boldsymbol{\sigma}(k)\\ \boldsymbol{\varsigma}(k)\end{matrix}\right\|, 1\right) \tag{48}$$

$$m_B(k+1) = \mu_{mB} m_B(k) + g_B \max\left(\|\boldsymbol{\delta}(k)\|, 1\right) \tag{49}$$

$$m_C(k+1) = \mu_{mC} m_C(k) + g_C \max\left(\|\varphi(k)\|, 1\right) \tag{50}$$

where $0 < \mu_m < 1$, $g > 0$, $\gamma > 0$, μ is step size, and $\|\bullet\|$ denotes the vector norm. $m(k)$ is the normalizing signal employed to stabilize the adaptation even in the presence of unmodelled dynamics (Ortega & Yu, 1987).

4.4 Overall structure of adaptive signal selection controller

The overall structure of the adaptive Signal Selection Controller in Fig. 4 and Fig. 5 is now given by combining the extractor in Fig. 6 and adaptive controllers $\hat{K}(z,k)$ in Fig. 7~10.
Fig. 11 shows one example of overall Necs-Extraction Controller, which is Fig. 4 type combining Fig. 6 and Fig. 10.

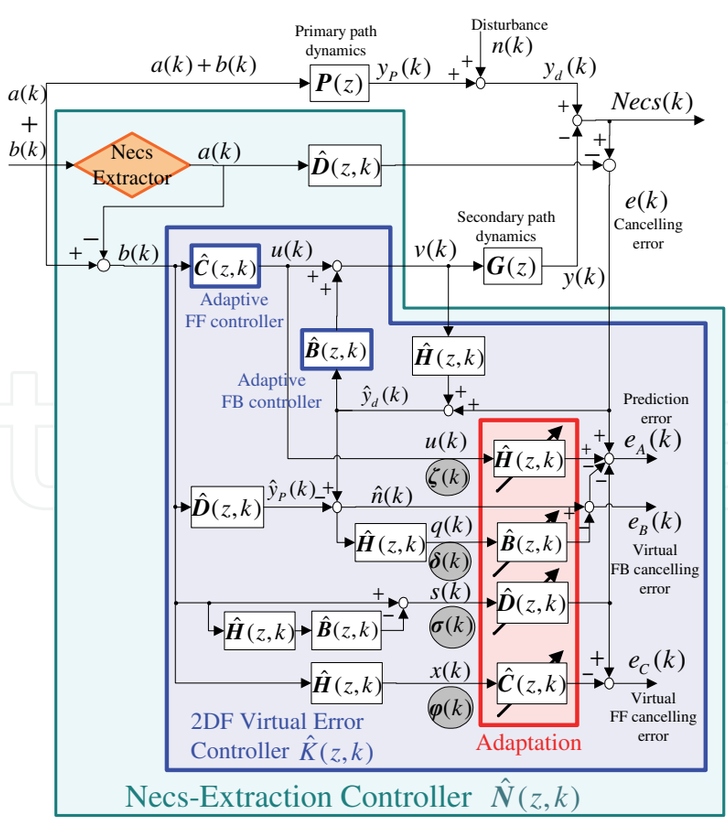

Fig. 11. One example of overall structure for Necs-Extraction Controller

5. Results of numerical simulations

To validate effectiveness of the proposed SSC, two applications to Sound Selection Systems (SSS) are considered as numerical simulations.

5.1 Numerical simulation of Necs-Extraction Control

First example is an application of the Necs-Extraction Controller to a smart window system (SWS) of a car, which can transmit only electronic siren sound of ambulance as Necs, but block any other noises such as road noise and engine noise. Purpose of this application is to keep car room silent and safety against car accidents at the same time.

In the simulation, we compare the results obtained by the four adaptive algorithms: (i) the filtered-X LMS approach (FX-SWS), (ii) the 2DF filtered-X LMS approach (2DF-FX-SWS), (iii) the Virtual Error approach (VE-SWS), and (iv) the proposed 2DF Virtual Error approach (2DF-VE-SWS). In the two filtered-X approaches, the modeling error of 20% in the filtered dynamics is considered. The simulation setup for the proposed method is summarized in Table 3.

Schemes	Design parameters
2DF-VE Controller	$L_d = 1, \mu_D = 0.220, L_H = 20, \mu_H = 0.23,$ $L_b = 5, \mu_B = 0.068, L_C = 30, \mu_C = 1.20,$ $\mu_{mA} = 0.4, g_A = 0.6, \gamma_A = 0.0006,$ $\mu_{mB} = 0.4, g_B = 0.6, \gamma_B = 0.0018,$ $\mu_{mC} = 0.4, g_C = 0.6, \gamma_C = 0.0220$
Extractor	$\mu = 0.03, \mu_{\omega\max} = 16, \mu_{\omega\min} = 4, N = 500, M = 4,$ $\omega = 20-650Hz, 650-1200Hz, 700-850Hz, 870-1060Hz$

Table 3. Design parameters of the 2DF-VE-SWS in simulations

In the simulation, it is assumed that the Necs $a(k)$ is set to the siren signal of a passing ambulance car at speed of 60km/h from 10 sec to 20 sec, the Unecs $b(k)$ is set to a unwanted stationary noise of 840Hz sinusoid with sound pressure level (SPL) of 90dB, and the unknown disturbance $n(k)$ is 100Hz sinusoid with SPL of 80dB.

Fig. 12 shows the four simulation results. Fig. 12 (a) gives $Necs(k)$ when uncontrolled, Fig. 12 (b) plots the estimated frequency by the extractor, Fig. 12 (c)-(f) compare the obtained profiles of $Necs(k)$ when controlled by each control approach. As shown in Fig. 12 (c) and (e), the FF control approaches cannot reduce the disturbance $n(k)$, though they can block the Unecs $b(k)$ and transmit the Necs $a(k)$. On the other hand, the proposed 2DF-VE-SWS can successfully reduce both disturbance $n(k)$ and Unecs $b(k)$ and transmit only the Necs $a(k)$, as in Fig. 12 (f), while the 2DF-FX-SWS based on the ordinary filtered-x algorithm cannot obtain stabilized results due to modeling errors as shown in Fig. 10 (d). Note that the scale of the vertical axis in Fig. 12 (d) is different from other figures. Fig. 12 (b) shows that the proposed extractor can estimate the frequencies of $a(k)+b(k)$ correctly, where large variations of the two estimated frequencies around 15 sec are due to passing of the ambulance. Consequently, it is validated that the performance of the proposed method 2DF-VE-SWS is the best in four controllers.

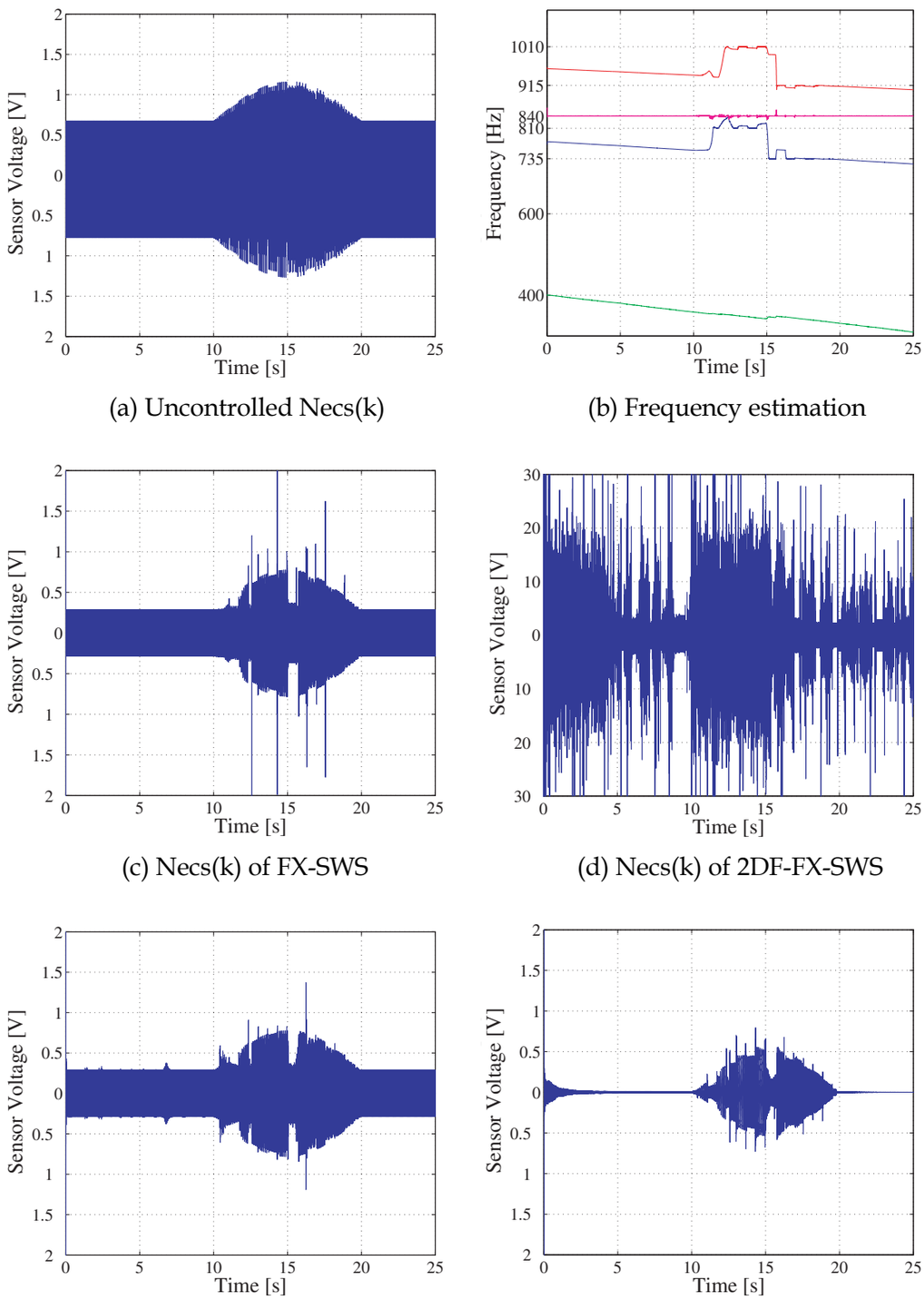

(a) Uncontrolled Necs(k)

(b) Frequency estimation

(c) Necs(k) of FX-SWS

(d) Necs(k) of 2DF-FX-SWS

(e) Necs(k) of VE-SWS

(f) Necs(k) of 2DF-VE-SWS

Fig. 12. Simulation results of four Necs-Extraction Controllers

5.2 Numerical simulation of Unecs-Canceling Control

Second example is another application of the Unecs-Canceling Controller to rotating machinery such as a compressor, which can attenuate only sound of rotating motor as Unecs even when rotating speed is changing, but transmit some abnormal sound of the machinery. Purpose of this application is to keep machinery silence and detectability of machine abnormality at the same time.

In the simulation, we will examine whether the Unecs-Canceling Controller works correctly or not. We consider the case that AC servo motor of a compressor starts to rotate from 0rpm at 0sec, and accelerate to 3600rpm until 10sec, then rotate constantly at 3600rpm after 10sec. Additionally, 240Hz abnormal sound of the machinery occurs from 8sec to 20sec.

And in this simulation, we consider the Unecs-Canceling Controller composed of 2-degree-of-freedom Virtual Error Controller, because the 2DF-VE controller shows the best performance in the simulation of Necs-Extraction Controller in section 5.1.

The simulation setup for the proposed method is summarized in Table 4.

Fig. 13 shows the simulation results. Fig. 13 (a) gives $Necs(k)$ when uncontrolled, Fig. 13 (b) shows the obtained profiles of $Necs(k)$ when controlled by 2DF-VE control approach, Fig. 13 (c) plots the estimated motor rotation speed by the extractor, and Fig. 13(d) describes the cancelling error.

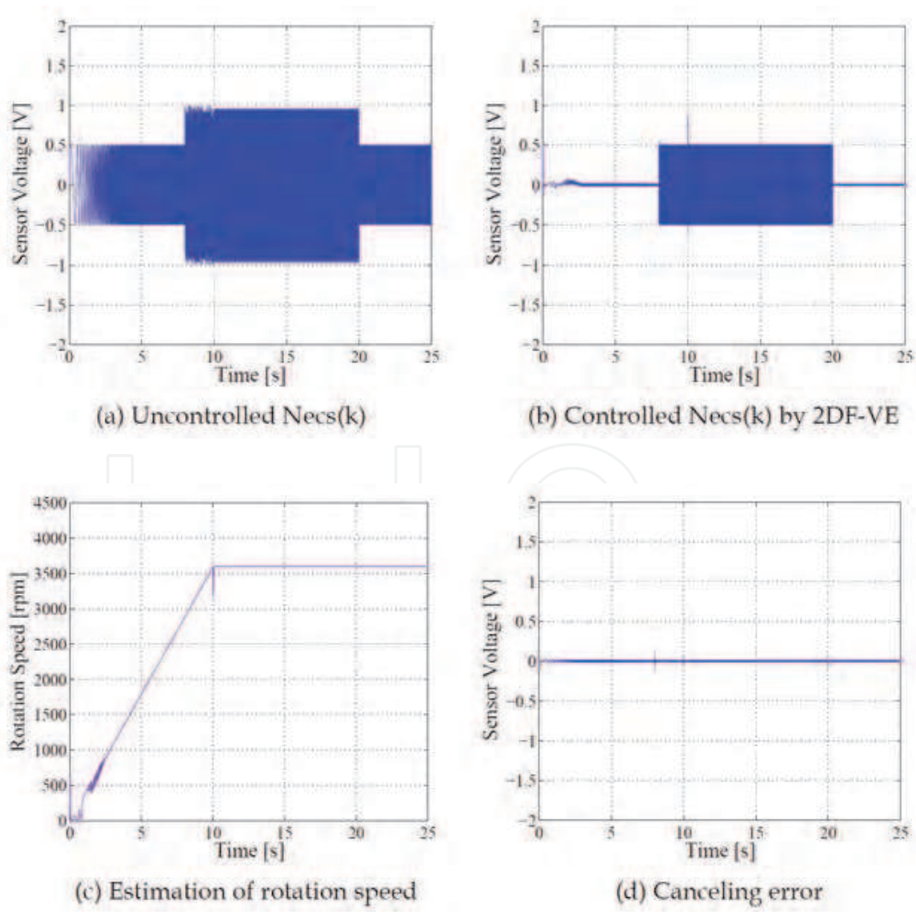

Fig. 13. Simulation results of Unecs-Canceling Controller

As shown in Fig. 13(b), the Unecs-Canceling Controller can attenuate motor sound, and transmit only abnormal sound of machinery from 8sec to 20sec. And Fig. 13(c) shows the good performance of the frequency estimation of the extractor. Besides, Fig. 13(d) shows that adaptation of the 2DF-VE controller is stable and rapid enough even if the frequency of extracting signal varies.
Consequently, it is validated that Unecs-Canceling Controller shows good performance to attenuate only desired signals.

Schemes	Design parameters
2DF-VE Controller	$L_d = 1, \mu_D = 0.220, L_H = 20, \mu_H = 0.23,$ $L_b = 5, \mu_B = 0.068, L_C = 30, \mu_C = 1.20,$ $\mu_{mA} = 0.4, g_A = 0.6, \gamma_A = 0.0006,$ $\mu_{mB} = 0.4, g_B = 0.6, \gamma_B = 0.0018,$ $\mu_{mC} = 0.4, g_C = 0.6, \gamma_C = 0.0220$
Extractor	$\mu = 0.03, \mu_{\omega\max} = 16, \mu_{\omega\min} = 4, N = 500, M = 4,$ $\omega = 0 - 650Hz, 200 - 300Hz, 300 - 600Hz, 600 - 1000Hz$

Table 4. Design parameters of the Unecs-Canceling Controller in simulations

6. Conclusion

We have proposed a novel control scheme which can transmit necessary signals (Necs) and attenuate only unnecessary signals (Unecs) selectively. The control scheme is named as Signal Selection Control (SSC) scheme.
Proposed control schemes are two types of the SSC; one is Necs-Extraction Controller which transmits only signals set as Necs, and the other is Unecs-Canceling Controller which attenuates only signals set as Unecs.
Besides, in the SSC, we have introduced four types of adaptive controller, and it is validated that the 2-degree-of-freedom Virtual Error controller has the best performance in the four adaptive controllers.
Consequently, effectiveness of both SSC are validated in two numerical simulations of the Sound Selection Systems.

7. Acknowledgment

This work was fully supported by Graduate School of Integrated Design Engineering, Keio University, Yokohama, Japan.

8. References

C. Bao and J. Pan, "Experimental study of different approaches for active control of sound transmission through double walls," *J. Acoust. Soc. Am.* , Vol. 102, No. 3, pp. 1664-1670, 1997.

J.C. Burgess, "Active adaptive sound control in a duct," *J. Acoust. Soc. Am.* , Vol. 70, No. 3, pp. 715-726, 1981.

A. Jakob and M. Möser, "Active control of double-glazed windows Part I: Feedforward control," *J. Applied Acoust.* , Vol. 64, pp. 163-182, 2003.

A. Jakob and M. Möser, "Active control of double-glazed windows. Part II: Feedback control," *J. Applied Acoust.* , Vol. 64, pp. 183-196, 2003.

O.E. Kaiser, S.J. Pietrzko and M. Morari, "Feedback control of sound transmission through a double glazed window," *J. Sound and Vibration*, Vol. 263, pp. 775-795, 2003.

T. Kohno and A. Sano, "Direct adaptive active noise control algorithms in case of uncertain secondary path dynamics, Int. *J. Adapt. Contr. Signal Process.* , Vol. 19, pp. 153-176, 2005.

S.M. Kuo, D.R. Morgan, *Active Noise Control Systems -Algorithms and DSP Implementations-*, Wiley. Interscience, 1996.

S.M. Kuo and D.R. Morgan, "Active noise control: a tutorial review," *Proc. The IEEE*, Vol. 87, No. 6, pp. 943-973, 1999.

S.O. Reza Moheimani, "A survey of recent innovations in vibration damping and control using shunted piezoelectric transducers," *IEEE Trans. Contr. Syst. Tech.* , Vol. 11, No. 4, pp. 482-494, 2003.

S.O. Reza Moheimani and A.J. Fleming, *Piezoelectric Transducers for Vibration Control and Damping*, Springer, 2005.

K.S. Narendra and A.M. Annaswamy, "Robust adaptive control in the presence of bounded disturbances," *IEEE Trans. Automatic Control*, Vol. AC-31, No. 4, pp. 306-315, 1986.

Y. Ohta and A. Sano, "Direct adaptive approach to multichannel active noise control and sound reproduction", P*roc. 2004 American Control Conference*, pp.2895- 2900, Boston, USA, 2004.

H. Okumura, R. Emi and A. Sano, "Adaptive two degree-of-freedom vibration control for flexible plate with piezoelectric patches," *Proc. SICE Annual Conf. 2008*, Tokyo, 1A09-5, pp. 218-221, 2008.

H. Okumura and A. Sano, "Adaptive Necessary Signal Extraction Controll Based on 2DF Virtual Error Approach to Smart Window Systems," *Proc. 48th IEEE Conf. on Desision and Control held jointly with 2009 28th Chinese Control Conf.* , Shanghai, China, ThC06. 4, pp. 5446-5453, 2009.

R. Ortega and T. Yu, "Theoretical results of robustness of direct adaptive controllers," *Proc. IFAC World Congress*, Munchen, 1987.

J. Pan and C. Bao, "Analytical study of different approaches for active control of sound transmission through double walls, *J. Acoust. Soc. Am.* , Vol. 103, No. 4, pp. 1916-1922, 1998.

P. Sas, C. Bao, F. Augusztinovicz and W. Desmet, "Active control of sound transmission through a double panel partition," *J. Sound and Vibration*, Vol. 180, No. 4, pp. 609-625, 1995.

Y. Shimada, Y. Nishimura, T. Usagawa and M. Ebata, "Active control for periodic noise with variable fundamental -an extended DXHS algotithm with frequency tracking ability -," *J. Acoust. Soc. Jpn. (E)*, Vol. 20, No. 4, pp. 301-312, 1999.

O. Tokhi and S. Veres, *Active sound and vibration control -theory and applications-*, The Institution of Electrical Engineers, 2002.

B. Widrow, D. Shur and S. Shaffer, "On adaptive inverse control," *Proc. the 15th Asilomar Conf. Circuits, Syst. Comput.* , Vol. 9, No. 11, pp. 185-189, Pacific Grove, CA1981-11, 1982.

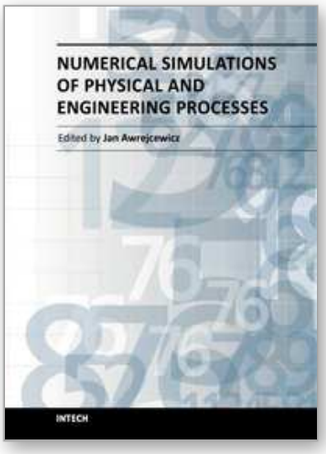

Numerical Simulations of Physical and Engineering Processes

Edited by Prof. Jan Awrejcewicz

ISBN 978-953-307-620-1

Hard cover, 594 pages

Publisher InTech

Published online 26, September, 2011

Published in print edition September, 2011

Numerical Simulations of Physical and Engineering Process is an edited book divided into two parts. Part I devoted to Physical Processes contains 14 chapters, whereas Part II titled Engineering Processes has 13 contributions. The book handles the recent research devoted to numerical simulations of physical and engineering systems. It can be treated as a bridge linking various numerical approaches of two closely inter-related branches of science, i.e. physics and engineering. Since the numerical simulations play a key role in both theoretical and application oriented research, professional reference books are highly needed by pure research scientists, applied mathematicians, engineers as well post-graduate students. In other words, it is expected that the book will serve as an effective tool in training the mentioned groups of researchers and beyond.

InTech Europe

University Campus STeP Ri

Slavka Krautzeka 83/A

51000 Rijeka, Croatia

Phone: +385 (51) 770 447

Fax: +385 (51) 686 166

www.intechopen.com

InTech China

Unit 405, Office Block, Hotel Equatorial Shanghai

No.65, Yan An Road (West), Shanghai, 200040, China

中国上海市延安西路65号上海国际贵都大饭店办公楼405单元

Phone: +86-21-62489820

Fax: +86-21-62489821